Fluorescent Polymersomes with Aggregation-Induced Emission

Nian Zhang, Hui Chen, Yujiao Fan, Lu Zhou, Sylvain Trépout, Jia Guo, Min-Hui Li

Fluorescent Polymersomes with Aggregation-Induced Emission

Nian Zhang,[a,†] *Hui Chen,*[b,†] *Yujiao Fan,*[b,†] *Lu Zhou,*[a] *Sylvain Trépout,*[c] *Jia Guo,*[a] *and Min-Hui Li* [a,b,*]

[a] Beijing Advanced Innovation Center for Soft Matter Science and Engineering, Beijing University of Chemical Technology, 15 North Third Ring Road, Chaoyang District, 100029 Beijing, P. R. China.

[b] Chimie ParisTech, PSL University Paris, CNRS, Institut de Recherche de Chimie Paris, UMR8247, 11 rue Pierre et Marie Curie, 75005 Paris, France.

[c] Institut Curie, INSERM U1196 and CNRS UMR9187, 91405 Orsay cedex, France.

[†] These authors contributed equally to this work.

[*] Corresponding Author: min-hui.li@chimieparistech.psl.eu

ABSTRACT.

Fluorescent polymersomes are interesting systems for cell/tissue imaging and in vivo study of drug distribution and delivery. We report on bright fluorescent polymersomes with aggregation-induced emission self-assembled by a series of tetraphenylethylene(TPE)-containing amphiphilic biodegradable block copolymers, where the hydrophilic block is a polyethyleneglycol PEG and hydrophobic block is a TPE-substituted trimethylenecarbonate polymer P(TPE-TMC). Their self-assemblies in water were prepared by nanoprecipitation using dioxane or THF as co-solvent, and the self-assembling processes were studied in detail by cryo-EM, DLS and spectrofluorometer. The polymersomes are formed via the closure of bilayer lamellae self-assembled first by amphiphilic block copolymers. The polymersome membrane affords a nanosize bright fluorescent system with self-assembly induced emission in the thickness scale of 10-15 nm. The control of whole size of polymersome is achieved by the choice of co-solvent for self-assembling and by the design of suitable hydrophilic/hydrophobic ratio of block copolymers. These polymersomes can be potentially used as a stable fluorescent tool to monitor the transportation and distribution of drugs and bioconjugates in living cells.

KEYWORDS. polymersomes, self-assembly, aggregation-induced emission, fluorescence, amphiphilic block copolymers.

Polymer vesicles, commonly called polymersomes, are spherical shell structures in which an aqueous compartment is enclosed by a bilayer membrane made from amphiphilic block copolymers.[1] This structure exhibits tremendously interesting properties such as high membrane elasticity and large encapsulation capacity. Polymersomes can entrap not only many hydrophilic molecules in the large volume of the inner aqueous compartment, but also a considerable quantity of hydrophobic molecules in the membrane of high molecular weight polymers (big hydrophobic pockets). Compared to liposomes, their low molecular weight analogues, polymersomes have been found to circulate in blood for much longer durations by merit of their tougher membranes and greater anti-fouling capacity.[2] Polymer chemistry also enables unlimited molecular design of site-targeted and stimuli-responsive polymersomes.[3-6] Therefore, with appropriate size, shape and chemistry, polymersomes would be capable of entering cells for cell-compartment imaging or releasing their cargo intracellularly. For these reasons, polymersomes are currently being studied as a means of drug delivery and biomedical imaging.[7-9] Fluorescent polymersomes are interesting systems for cell/tissue imaging and *in vivo* study of drug distribution and delivery. Traditional fluorescent polymersomes contain generally conventional organic dyes which suffer from aggregation-caused quenching (ACQ).[10] It will be very interesting to develop fluorescent polymersomes composed of luminogens with aggregation-induced emission (AIE) characteristics that have emerged since last decade as alternative fluorescent materials for organelles imaging and drug delivery monitoring.[11-14] The combination of AIEgens with polymersomes, will provide innovative approaches for bioimaging and theranostics. However, as far as we are aware, only a few studies on AIE polymersomes have been reported.[15-21]

In this paper we report on fluorescent polymersomes with AIE properties prepared from amphiphilic block copolymer PEG-*b*-P(TPE-TMC), where the hydrophobic block P(TPE-TMC) is a tetraphenylethylene(TPE)-containing poly(trimethylene carbonate) (PTMC). The hydrophobic polymers based on PTMC are extensively studied for biomedical applications because of their special degradation behavior such as resistance to non-enzymatic hydrolysis, generation of non-acidic degradation products, and enzymatic degradation with a surface erosion mechanism.[22, 23] Polymersomes made of PTMC-containing amphiphilic block copolymers have also been reported.[24, 25] In this study we connect the emblematic, propeller-shaped AIEgen, TPE, to each monomer of PTMC. PTMC-based polymers can be prepared by a ring-opening polymerization (ROP) of 6-membred trimethylene carbonate (TMC) using a variety of catalysts including conventional organometallic catalysts or other metallic complex catalysts,[26] and emerging organocatalysts.[27-30] The recent development of biocompatible polymers free of potentially toxic metallic components has promoted the search for organic catalytic and initiating systems.[30, 31] Especially, the organocatalytic system based on acid-base pairs, such as N-(3,5-trifluoromethyl)phenyl-N′-cyclohexylthiourea (TU) and 1,8-diazabicyclo[5.4.0]undec-7-ene (DBU), has emerged as a versatile catalyst and demonstrated to have good control over polymerization as well as tolerance to numerous functional groups.[28, 31] Hence, in this study we performed the polymerization of the TPE-functionalized 6-membred cyclic carbonate monomer (TPE-TMC) using TU-DBU pair as organocatalyst and commercial methoxy-polyethyleneglycol ($mPEG_{45}$-OH) as macroinitiator. Amphiphilic diblock copolymers PEG_{45}-*b*-$P(TPE\text{-}TMC)_n$ with different hydrophobic block ratios were prepared in order to study their influence on the size and morphology of the self-assemblies. The self-assembling behaviors and AIE fluorescence properties of one of the copolymers, PEG_{45}-*b*-$P(TPE\text{-}TMC)_{13}$ (f_{PEG} = 21 wt%) with

hydrophilic/hydrophobic weight ratio of 21/79, was studied in detail as an example. Cryo-EM, DLS and spectrofluorometer allow the monitoring of the self-assembling process, and a mechanism of type I[26] was revealed, where the polymer vesicles were formed by the closure of large bilayer lamellae of amphiphilic block copolymers. Well-structured fluorescent polymersomes were successfully achieved. The simple AIEgen-containing diblock copolymers reported here provide direct access to AIE polymersomes in aqueous conditions. The biocompatible and biodegradable nature of the block copolymer backbone renders these AIE polymersomes attractive for the future application in drug delivery and biomedical imaging.

RESULTS AND DISCUSSION

Monomer and polymer synthesis. The monomer TPE-TMC was first synthesized from 2,2-bis-(hydroxymethyl) propionic acid (bis-MPA) according to the literature.[31-34] The synthetic routes of monomer and polymers are shown in Scheme 1. The monomer **5** (also simply named as TPE-TMC) was synthesized with five steps in high yield. Briefly, the compound **1** was first prepared by coupling reaction of diphenylmethane with 4-methoxybenzophenone, followed by acid-catalyzed dehydration and de-protection reaction.[35] By two Williamson reactions, the compound **3** was connected to 2,2-bis(hydroxymethyl)propionic acid and provided the precursor diol **4**, which was then cyclized with triphosgene in the presence of pyridine to afford the monomer **5** (TPE-TMC). All the compounds were carefully purified and characterized by ^{1}H NMR and ^{13}C NMR (spectra shown in Figure S1-S5 of the Supporting Information).

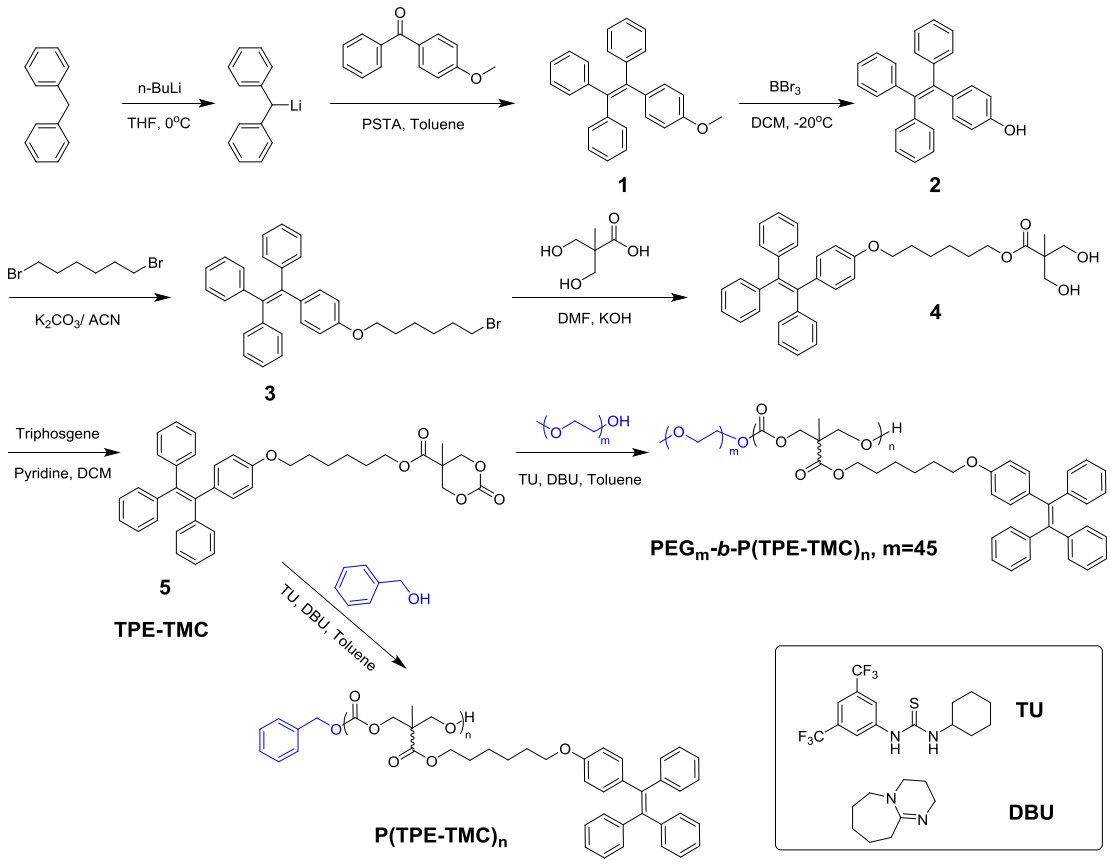

Scheme 1. Synthetic route of tetraphenylethene-functionalized monomer 5 (TPE-TMC) and its homopolymer P(TPE-TMC)$_n$ and diblock copolymer PEG$_{45}$-*b*-P(TPE-TMC)$_n$.

The homopolymerization of monomer **5** (TPE-TMC) was conducted using benzyl alcohol as initiator and TU/DBU as catalysts, resulting in TPE-containing polymers with predictable molecular weights and relatively low PDI. The commercially available mPEG$_{45}$-OH (M_n = 2000 Da) was then employed as the macroinitiator to readily prepare a series of AIE amphiphilic diblock copolymers PEG$_{45}$-*b*-P(TPE-TMC)$_n$. The reaction kinetics of ROP of monomer TPE-TMC with mPEG$_{45}$-OH as initiators was first studied (see Supporting Information, Figure S6). A monomer conversion of 80% was obtained in ~1 h. We observed a linear increase of ln[M]$_0$/[M] with time when the conversion is below 80%. This showed that the polymerization of TPE-TMC

was controlled and had a first-order kinetics at conversions lower than 80%. From the slope of $\ln[M]_0/[M]$ vs. time, the apparent propagation rate constants can be obtained, k_{app} = 0.017 s^{-1}. The molecular weight increased also linearly and polydispersity remained low (< 1.35). We then kept the monomer conversion lower than 80% to synthesize amphiphilic copolymer with predictable molecular weights. The hydrophilic block's weight ratios (f_{PEG}) were designed from 15 to 40 wt% according to the reference values of lipids in liposomes (~ 35 wt%) and those of polymersome-forming amphiphilic block copolymers with complex hydrophobic block (*e.g.*, mesogen-containing block) (15 – 40 wt%).[36] A series of AIE amphiphilic diblock copolymers PEG_{45}-*b*-$P(TPE\text{-}TMC)_n$ (n = 16, 13, 9, 7) with relatively low PDI were obtained as shown in Table 1. All polymers were carefully purified and characterized by ^1H NMR and SEC with spectra shown in Figure S9-S12 of the supporting information.

Table 1. Molecular weights and molecular weight distributions of homopolymer $P(TPE\text{-}TMC)_n$ and PEG_{45}-*b*-$P(TPE\text{-}TMC)_n$ diblock copolymers

Polymer sample	DP of hydrophobic block (n) [a]	M_n (Da) [a]	PDI [b]	f_{PEG} (wt%) [a]
$P(TPE\text{-}TMC)_{24}$	24	14100	1.35	-
PEG_{45}-*b*-$P(TPE\text{-}TMC)_{16}$	16	11400	1.30	17
PEG_{45}-*b*-$P(TPE\text{-}TMC)_{13}$	13	9600	1.35	21
PEG_{45}-*b*-$P(TPE\text{-}TMC)_9$	9	7300	1.32	27
PEG_{45}-*b*-$P(TPE\text{-}TMC)_7$	7	6100	1.26	33

[a] The degree of polymerization (DP) of the hydrophobic block (P(TPE-TMC)) and the number average molecular weight (M_n) and the hydrophilic weight ratio (f_{PEG}) of the copolymer were determined by ^1H NMR spectroscopy (Detail method see in Figure S8). The molecular weight of monomer TPE-TMC is 590.72 Da.

[b] PDI = M_w/M_n, M_w and M_n here were measured by SEC using THF as eluent and monodispersed polystyrenes as calibration standards.

Thermal and AIE properties of the homopolymer. The homopolymer was first studied by DSC to measure the possible phase transitions. Figure 1A shows the DSC curve of P(TPE-TMC)$_{24}$ in which only a T_g at 35.5°C is measured. This indicates that this TPE-containing poly(trimethylenecarbonate) homopolymer presents a glassy amorphous state at room temperature.

The UV-visible absorption spectra of the monomer and the homopolymer P(TPE-TMC)$_{24}$ in THF and dioxane were measured, respectively. Figure 1B shows the spectra in THF, and those in dioxane are very similar (not shown). A large absorption peak with a maximum around 318 nm was observed in all cases in both solvent, which is characteristic of TPE moiety. Then the AIE properties of P(TPE-TMC)$_{24}$ were checked by monitoring its fluorescence intensity as it was solubilized or dispersed in the solution with different composition of solvents. THF and dioxane were chosen as organic solvents because they were also the co-solvents used in the formation of polymersomes by nanoprecipitation (see next section). A mixture of water and THF (or dioxane) with different water fraction (f_w), namely 0%, 30%, 60%, 90%, 99%, was added, respectively, to each of five flasks that contained a tiny volume of homopolymer solution in THF (or dioxane) (v = 0.16 mL and c = 1.5 wt%), until a volume of 25 mL leading to 1x10^{-5} M polymer solution (0.0096 wt%). As shown in Figure 1C and 1D, homopolymer P(TPE-TMC)$_{24}$ exhibits obvious aggregation-induced emission characteristic when dispersed in water. Nevertheless, different behaviors were recorded between using THF and using dioxane as organic co-solvent. At f_w = 0, the homopolymer in THF or dioxane solution is non-emissive because it is perfectly soluble and the intramolecular rotation of TPE leads to non-radiative decay after UV illumination. At f_w = 30% in dioxane/H_2O mixture, the fluorescence starts to appear, while at the same f_w in THF/H_2O mixture the fluorescence is still not detectable.

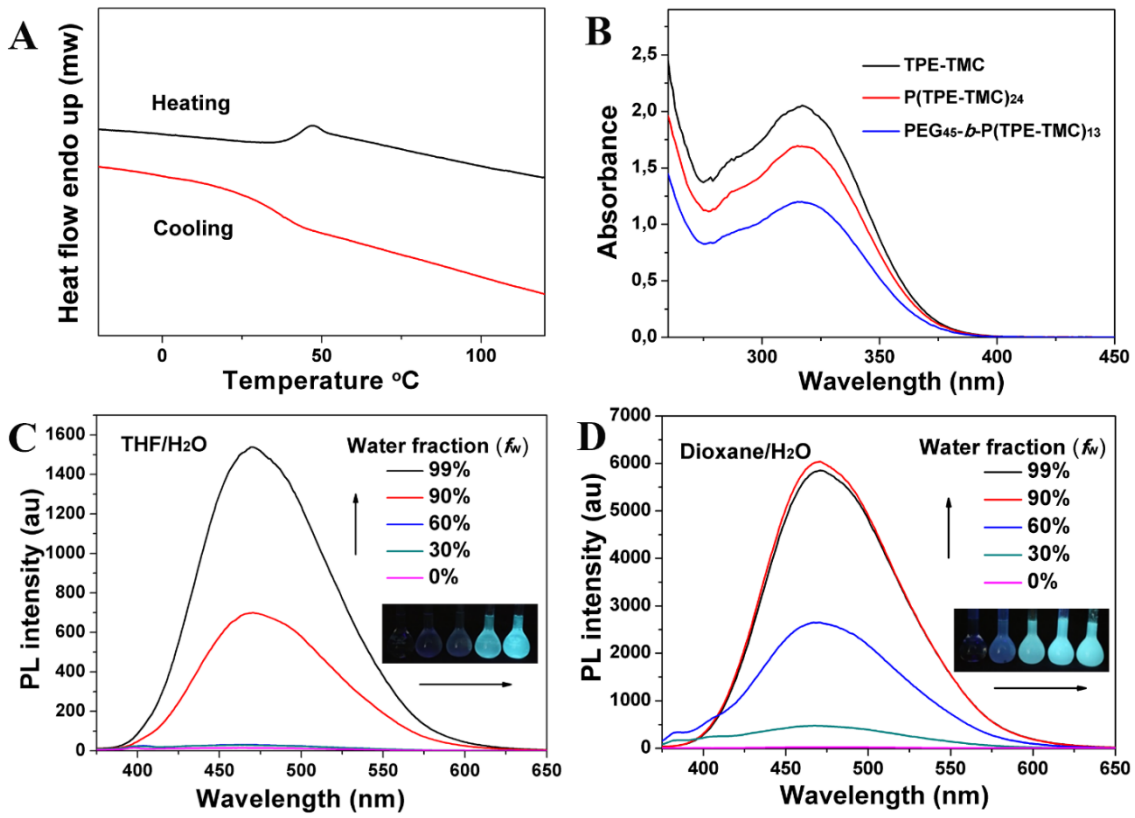

Figure 1 (A) DSC curves of the homopolymer P(TPE-TMC)$_{24}$ recorded at 10°C/min; (B) UV-vis absorption spectra of TPE-TMC, P(TPE-TMC)$_{24}$ and PEG$_{45}$-*b*-P(TPE-TMC)$_{13}$ in THF (concentration of polymer = 1x10^{-5} M, concentration of monomer = 1x10^{-4} M). (C) and (D) Photoluminescence (PL) spectra of P(TPE-TMC)$_{24}$ in THF/H_2O (C) mixtures and in dioxane/H_2O mixtures (D) with different water fractions (Concentration: 1x 10^{-5} M; excitation wavelength: 355nm; The two inserted photographs in (C) and (D) correspond to the photos when the different water fraction mixture exposure to UV light of 365 nm.). At f_w = 99% in dioxane/H_2O mixture (D), some aggregated samples precipitated from the solution, that explains why the fluorescence intensity of the dispersion is lower compared to that at f_w = 90%.

This is due to the difference of solubility of P(TPE-TMC)$_{24}$ in dioxane and in THF. At f_w = 30% in dioxane/H_2O the homopolymer starts to aggregate and to light up the fluorescence *via* the

restriction of the intramolecular motion of TPE moieties, while at the same water fraction in THF/H_2O the homopolymer dissolves still well showing no obvious fluorescence. The fluorescence intensity increases significantly as water fraction reaching 60% in dioxane/H_2O and 90% in THF/H_2O. In nearly pure water (f_w = 99%), the aggregates of the homopolymer in both cases show bright AIE fluorescence (Figure 1C and 1D).

Self-assembly of amphiphilic block copolymers PEG_{45}-*b*-P(TPE-TMC)$_n$. The method of nanoprecipitation was used to make the self-assemblies of the diblock copolymers PEG_{45}-*b*-P(TPE-TMC)$_n$ in water using THF or dioxane as co-solvent. Typically, the diblock copolymer was dissolved in 1 mL of THF or dioxane, a common solvent for both polymer blocks, at a concentration of 0.25 wt%. Deionized water was then added to the solution very slowly (2–3 μL of water per minute) with slight shaking. When the water content reached 75% where the formation of nanostructure already finished (see below), the dispersions of self-assemblies were dialyzed thoroughly against water to get final polymer self-assemblies in pure water. We have followed the self-assembly process *in-situ* upon water addition using DLS and cryo-EM in order to understand the self-assembling mechanism. We have focused especially on the self-assembling process of one block copolymer, PEG_{45}-*b*-P(TPE-TMC)$_{13}$ (f_{PEG} = 21wt%) in THF/water and in dioxane/water. The average size of the nanostructures and the count rates were regularly measured by DLS (Zetasizer). At some critical points, aliquots were taken to be frozen for cryo-EM analyses.

We discuss first the case using THF as co-solvent. Figure 2A shows the count rates (kcps) and the average hydrodynamic diameters (D_h) of aggregates as a function of water content in THF/water system. The count rates measured by Zetasizer in kilo counts per second (kcps) represent the scattering intensity. The higher count rate usually indicates higher concentration,

larger particles, or higher concentration and larger particles. We have recorded three events involved in the evolution of aggregates in the self-assembling process (Figure 2A). The first one corresponds to the appearance of very large structures with D_h up to 3 μm at water content of 20-25%. However only a small peak of count rates (peak value 230 kcps) was accordingly recorded, that means the concentration of these large structure is low. These large structures are probably large lamellae and giant vesicles formed by the closure of the lamellae. Indeed, cryo-EM made on aliquot withdrawn at water content of 25% showed giant vesicles (Figure 2C). The second event is an abrupt increase of count rates from 230 to 4000 kcps at water content from 32 to 36%. This event is ascribed to the sudden increase of the concentration of self-assemblies because in contrast the size of self-assemblies decreases to 200-300 nm at these water contents. The morphology was checked by cryo-EM on aliquot withdrawn at 31% of water content just before the abrupt change. The cryo-EM image (Figure 2D) shows indeed that the giant vesicles transform into smaller ones. The third event is the stabilization of the size and the concentration of self-assemblies as water content increased from 36% to 75% as shown in Figure 2A. The average D_h of 270 nm was measured and the count rates reached plateau value. The cryo-EM images of polymersomes at 75% of water content (Figure 2E) confirm the size of self-assemblies. The size distribution of polymersomes measured by DLS at three representative points (f_w = 25, 31, 75 % in the THF/water mixture) are collected in Figure 2B. Finally, the polymersomes in pure water were achieved by dialysis of the above mixture against water. The size distribution of polymersomes in pure water changed only very slightly compared to that in the mixture with f_w = 75% (see Figure S13), the average vesicles size of 250 nm (PDI = 0.133) being measured by DLS. Their cryo-EM images shown in Figure 3A confirm the well-defined vesicular structures of PEG_{45}-*b*-$P(TPE\text{-}TMC)_{13}$ in water using THF as co-solvent.

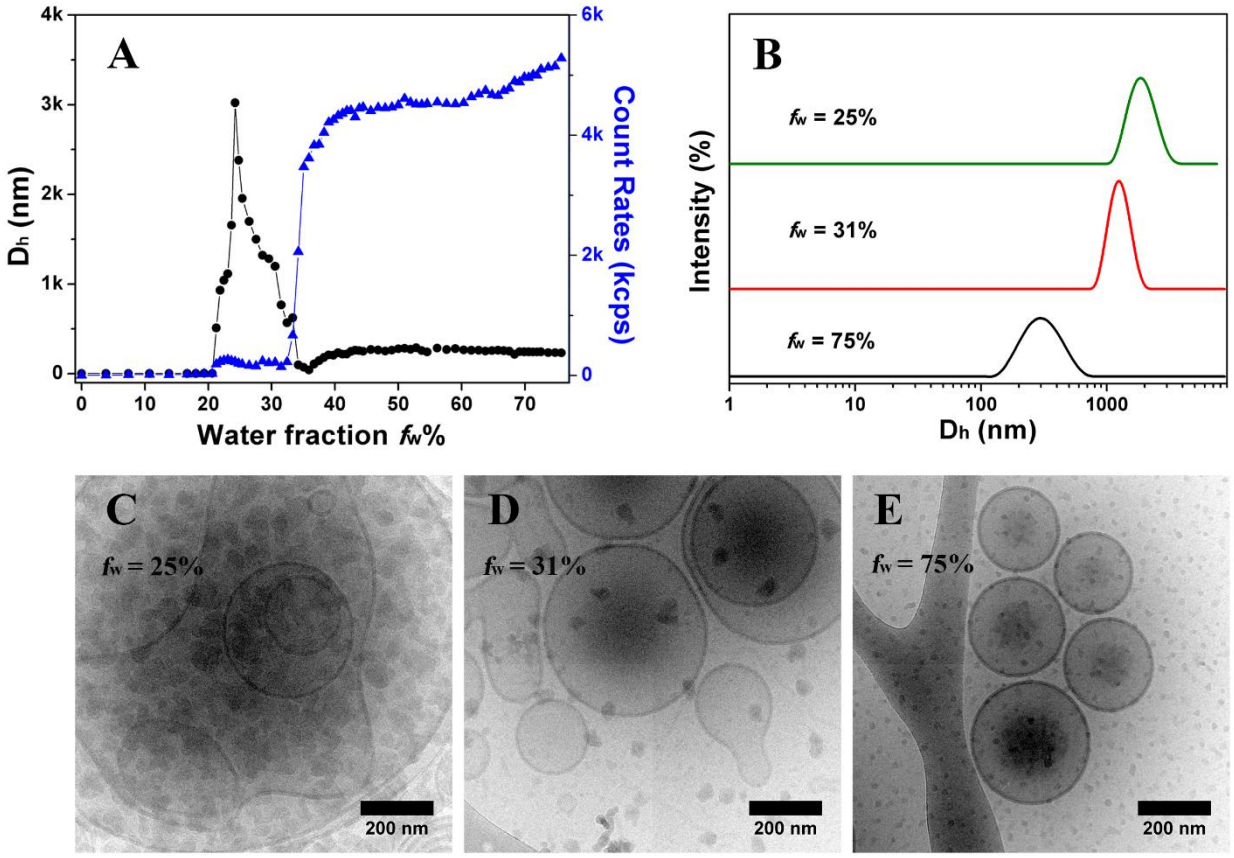

Figure 2. Study of the self-assembling process of PEG_{45}-*b*-P(TPE-TMC)$_{13}$ by nanoprecipitation in THF/water. (**A**): The evolution of average hydrodynamic diameter (D_h) and count rates measured by DLS as a function of water content upon water addition. (**B**): The size distribution of self-assemblies measured by DLS at water content f_w = 25%, 31%, 75%. (**C**)-(**E**): The cryo-EM images of self-assemblies at the water fraction f_w = 25% (**C**), 31% (**D**), and 75% (**E**). The dark spots in the cryo-EM images come from organic solvent (THF), because the samples were frozen in solvent mixtures.[37]

Dioxane was also used as organic co-solvent to do the self-assembling of PEG_{45}-*b*-P(TPE-TMC)$_{13}$. Figure S14 shows the average hydrodynamic sizes (D_h) and the count rates (kcps) of self-assemblies measured by DLS as a function of water content in dioxane. Similar evolution of

self-assemblies was observed for count rates and D_h as compared to the case using THF as co-solvent. However, the critical water fractions for the first and second events advanced in dioxane/water than those in THF/water. The big structures (sheets or giant vesicles) appeared at f_w = 10% in dioxane/water instead of appearing at f_w = 20% in THF/water; a lot of vesicles (high concentration) started to form with abrupt increase of count rates at f_w = 20% in dioxane/water instead of forming at f_w = 35% in THF/water. In addition, the final polymersomes have sizes much larger than those obtained in THF/water system. When the water content reached 75%, vesicles stabilized its size at 700 nm. Large vesicles with average diameters of 650 nm (PDI = 0.137) were observed after the self-assembled solution was dialyzed against water (Figure S15). Their cryo-EM images shown in Figure 3B confirm the structures of the big vesicles.

These different results indicate the solubility of amphiphilic block polymers in THF is better than in dioxane. This is in agreement with the solubility difference of homopolymer P(TPE-TMC) observed in THF and in dioxane as discussed above (**AIE properties of the homopolymer**). In order to understand better the different effects of THF and dioxane on self-assembling behavior of block copolymers, we examine the Flory–Huggins interaction parameters of these polymer-solvent pairs ($\chi_{p\text{-}s}$). Generally, if $\chi_{p\text{-}s} < 0.5$, the solvent dissolves well the polymer, whereas if $\chi_{p\text{-}s} > 0.5$, the solvent is poor for the polymer (for theta solution $\chi_{p\text{-}s} = 0.5$). Lower value of $\chi_{p\text{-}s}$ indicates better miscibility between polymer and solvent. $\chi_{p\text{-}s}$ can be calculated using the van Laar-Hildebrand equation (1):[38]

$$\chi_{p-s} = \frac{V_S}{\mathrm{RT}}\left(\delta_p - \delta_s\right)^2 + 0.34 \qquad (1)$$

where V_S is the molar volume of the solvent, R refers to the ideal gas constant, and T is temperature. δ_p and δ_s are the solubility parameters of polymer and solvent, respectively. The

term 0.34 gives the entropic contribution and is usually between 0.3 and 0.4 for non-polar system. The hydrogen bond effect is neglected in the PEG block. Solubility parameter (δ/MPa$^{1/2}$) for solvents are δ_{THF} =19.4 and $\delta_{dioxane}$ = 20.5, as calculated by Hansen *et al*.[38] Group contribution method is used to calculate the solubility parameter for polymers: δ_{PEG} = 20.2, $\delta_{P(TPE\text{-}TMC)}$ = 17.5. We found then $\chi_{PEG\text{-}THF}$ = 0.37, $\chi_{PEG\text{-}dioxane}$ = 0.34, $\chi_{P(TPE\text{-}TMC)\text{-}THF}$ = 0.43, $\chi_{P(TPE\text{-}TMC)\text{-}dioxane}$ = 0.61. These values indicate that THF and dioxane are nearly equivalently good solvent for PEG, while THF is clearly a better solvent for P(TPE-TMC) than dioxane. Therefore, as the selective solvent, water, that is a non-solvent for P(TPE-TMC) but good solvent for PEG, was added to the block copolymer solution in THF or dioxane, the aggregates appeared earlier (with lower water content) in dioxane than in THF. If we consider the interaction parameter between polymer unit is $\chi_{P(TPE\text{-}TMC)\text{-}P(TPE\text{-}TMC)}$ = 0.34, the interaction between THF and P(TPE-TMC) ($\chi_{P(TPE\text{-}TMC)\text{-}THF}$ = 0.43) is not so different from the interaction between P(TPE-TMC) and P(TPE-TMC). Then the membrane may contain plenty of THF. In contrast, the interaction between dioxane and P(TPE-TMC) with $\chi_{P(TPE\text{-}TMC)\text{-}dioxane}$ = 0.61 is not favorable compared to $\chi_{P(TPE\text{-}TMC)\text{-}P(TPE\text{-}TMC)}$ = 0.34 for the miscibility. Then upon water addition the interaction between P(TPE-TMC) and P(TPE-TMC) may be favored and the content of dioxane may be less in the membrane of dioxane/water system. The polymer membrane plasticized by more solvent (THF) should present better flexibility and lower bending modulus, leading to the formation of smaller vesicles. This may explain the final size difference between polymersomes obtained with THF/water and dioxane/water systems.

We analyze now the molecular organization in the polymersomes membrane. The membrane thickness of final vesicles dispersed in water obtained in both THF/water and dioxane/water systems remained the same and homogeneous in all vesicles. It was measured as 10 ± 1 nm from

the FWHM of the electronic density profile perpendicular to the membrane through statistical analysis of about 30 different vesicles in the cryo-EM images. This thickness corresponds to the hydrophobic part of the bilayer. PEG_{45}-*b*-$P(TPE\text{-}TMC)_{13}$ should have a tail-to-tail (P(TPE-TMC) to P(TPE-TMC)) bilayer structure in the bilayer membrane. As the molecular length of one TMC unit at the extended state in the polymer backbone is about 0.6 nm (calculated by Chem3D software), the biggest length of P(TPE-TMC) block in PEG_{45}-*b*-$P(TPE\text{-}TMC)_{13}$ should be 7.8 nm. A perfect tail-to-tail bilayer should have the membrane thickness of 15.6 nm. The measured membrane thicknesses of about 10 nm is smaller than the double length of P(TPE-TMC) block at the extended state. This indicates that in the vesicle membrane the PEG_{45}-*b*-$P(TPE\text{-}TMC)_{13}$ backbone may not be totally extended, or the two leaflets may be interdigitated and don't form an exact tail-to-tail bilayer (Figure 3D).

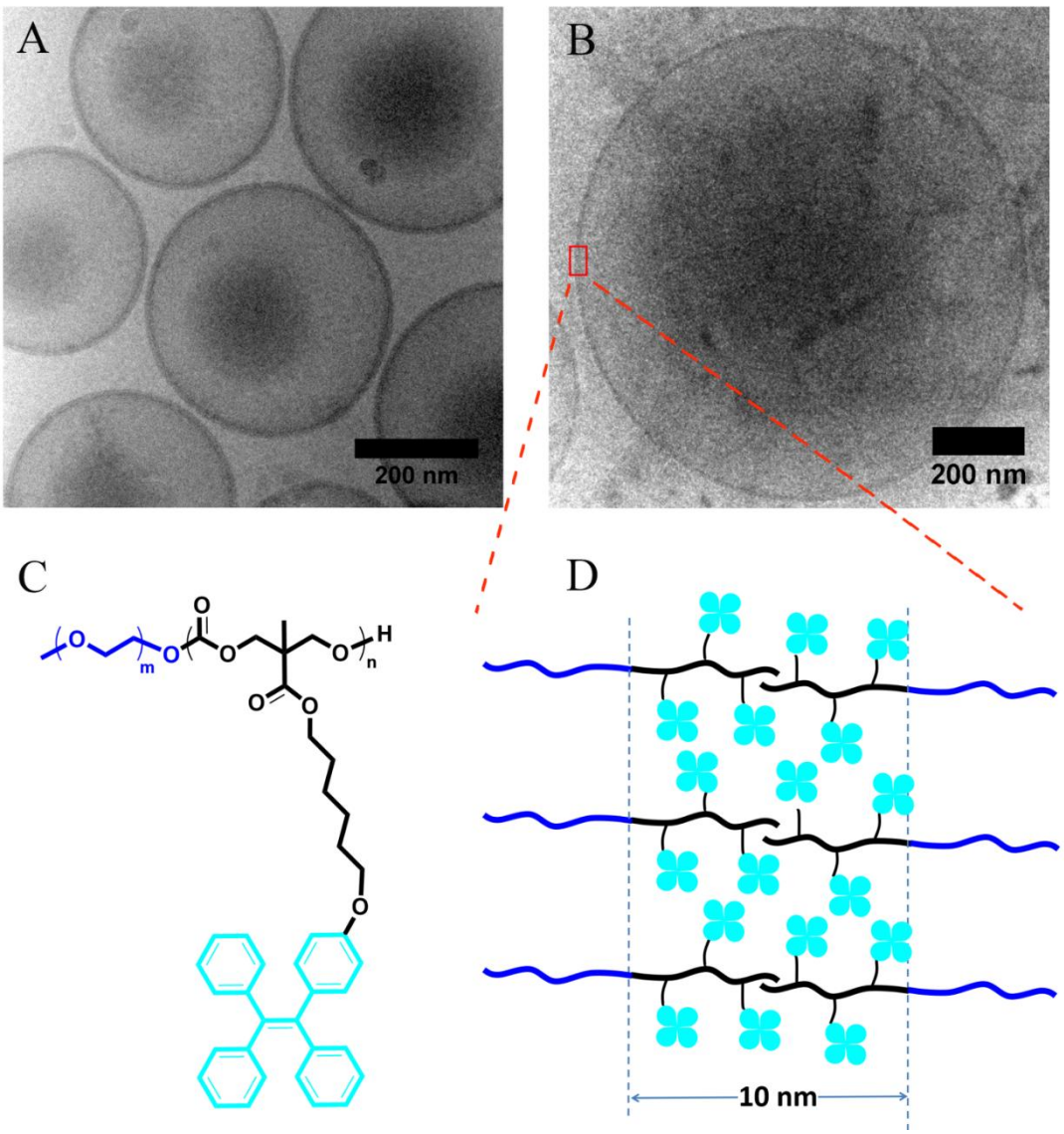

Figure 3. Cryo-electron micrographs of polymersomes formed by PEG_{45}-*b*-$P(TPE\text{-}TMC)_{13}$ in water by nanoprecipitation using THF (A) or dioxane (B) as co-solvent. The chemical structure of the block copolymer is shown in C and the schematic molecular organization in the membrane in D.

The self-assemblies of other block copolymers in Table 1 (PEG_{45}-*b*-$P(TPE\text{-}TMC)_n$, n = 16, 9, 7, with hydrophilic weight ratios f_{PEG} = 17%, 27%, 33%, respectively) were also prepared using THF/water as co-solvents. The final self-assemblies were obtained in water after thorough

dialysis against water. Figure 4 shows their size distributions measured by DLS and their morphologies imaged by cryo-EM. Table 2 lists the hydrodynamic diameters and membrane thicknesses of the polymersomes obtained by the whole series. With the decrease of the hydrophobic block length and the increase of the hydrophilic ratio, the average size of polymersomes becomes smaller (from D_h = 450 nm, 250 nm, 90 nm to 70 nm) and the average membrane thickness becomes thinner (from e =15.0 nm to 9.8 nm). It is easy to understand that shorter the hydrophobic block, thinner the membrane (see Figure 3D). The bending modulus of the membrane should depend on the whole molecular size of the block copolymer. It should be higher for membrane made of high molecular weight polymer than that made of low molecular weight polymer. This explains why the vesicles sizes are bigger for PEG_{45}-*b*-P(TPE-TMC)$_n$ with bigger n.[39, 40] Note that a few of big sheets and giant vesicles were also observed for shorter copolymers PEG_{45}-*b*-P(TPE-TMC)$_9$ and PEG_{45}-*b*-P(TPE-TMC)$_7$ (Figure S16). As all these assemblies formed by block copolymer in water *via* solvent exchange (nanoprecipitation) are kinetically trapped, vesicle closure may not be completed for the more flexible membranes with thinner thickness in the time scale used. Therefore, some of intermediate self-assemblies (sheets and giant vesicles) could remain at the end.

Table 2. The sizes of polymersomes self-assembled from PEG_{45}-*b*-P(TPE-TMC)$_n$ by nanoprecipitation using THF/water as co-solvents

Block copolymer	f_{PEG} (wt%)	D_h (nm) [a]	e (nm) [b]
PEG_{45}-*b*-P(TPE-TMC)$_{16}$	17	450	15.0 ± 1.5
PEG_{45}-*b*-P(TPE-TMC)$_{13}$	21	250	10.1 ± 1.0
PEG_{45}-*b*-P(TPE-TMC)$_9$	27	90	9.9 ± 1.1
PEG_{45}-*b*-P(TPE-TMC)$_7$	33	70	9.8 ±1.0

[a] Intensity average hydrodynamic diameters measured by DLS.

[b] Thickness measured from the FWHM of the electronic density profile perpendicular to the membrane through statistical analysis of about 30 different vesicles in the cryo-EM images.

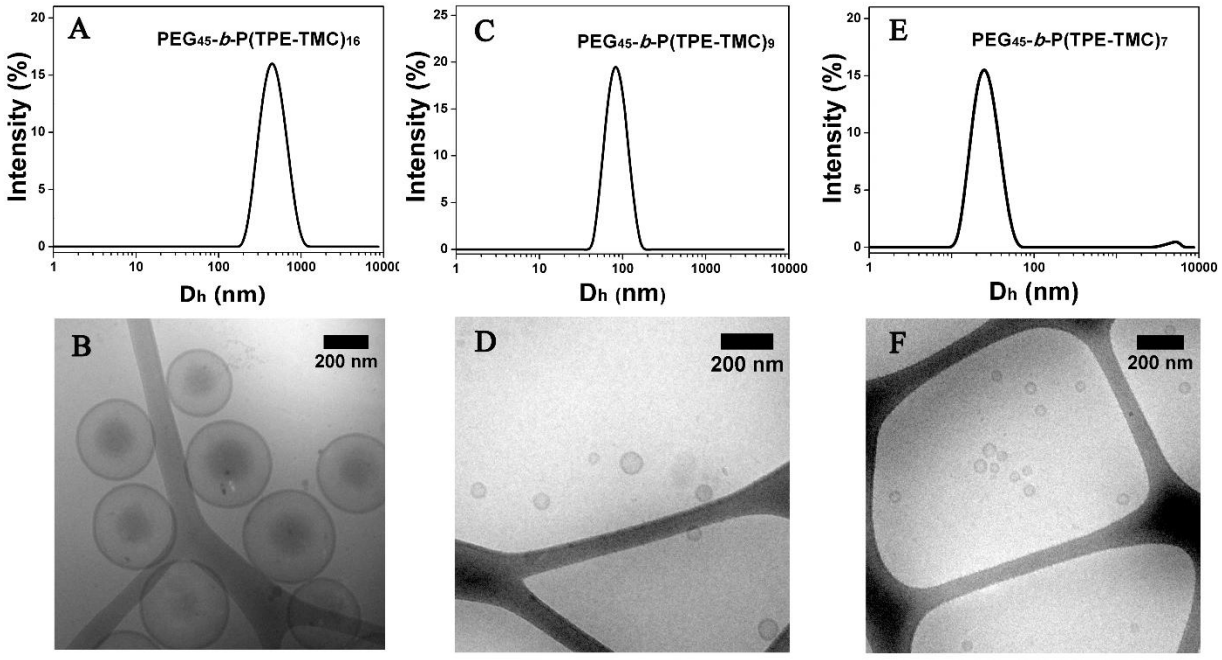

Figure 4. Characterization of polymersomes in water formed by PEG_{45}-*b*-P(TPE-TMC)$_n$ using nanoprecipitation in THF/water mixture. (A), (C) and (E) show their size (D_h) distribution measured by DLS; (B), (D) and (F) their Cryo-EM images. (A) and (B): PEG_{45}-*b*-P(TPE-TMC)$_{16}$

(f_{PEG} =17%). (C) and (D): PEG_{45}-*b*-P(TPE-TMC)$_9$ (f_{PEG} =27%). (E) and (F): PEG_{45}-*b*-$PMTC_7$ (f_{PEG} =33%).

In conclusion, we have demonstrated that the polymersomes were formed *via* a mechanism of type I[26], where amphiphilic block copolymers self-assembled first into large bilayer lamellae followed by the closure of lamellae to vesicles and transformation of giant vesicles to smaller vesicles. This mechanism can ensure high loading capacity of hydrophilic molecules inside the aqueous compartments. We have also empirically controlled the size of polymersomes by the choice of co-solvent (THF or dioxane) and by the design of suitable hydrophilic/hydrophobic ratio of the block copolymers. The size of polymersomes is an important parameter because it can influence the cell uptake of polymersomes.[41]

Aggregation-induced emission properties of polymersomes during the self-assembling. We have followed the fluorescence evolution of the polymersomes of PEG_{45}-*b*-P(TPE-TMC)$_{13}$ all through their formation. To choose the excitation wavelength, the excitation spectra of the self-assemblies of PEG_{45}-*b*-P(TPE-TMC)$_{13}$ in THF and in dioxane at f_w = 50% were first measured, which show a maximum at 382 nm (see Figure S17 for the spectrum in THF/H_2O). Then, the fluorescence intensity was measured by spectrofluorometer using excitation wavelength of 382 nm just after each water addition and DLS measurement during the above-discussed nanoprecipitation process. Figure 5 shows the fluorescence intensity evolution of the polymersome dispersion in THF/water and in dioxane/water systems. We can distinguish two main stages in the evolution of fluorescence intensity during the self-assembling process. Initially, there is a slight linear increase of fluorescence intensity as water content f_w changes from 20% to 60% in THF/H_2O system, and from 20% to 50% in dioxane/water system, respectively. Then, as f_w > 60% in THF/water or f_w > 50% in dioxane/water, the fluorescence

intensity increases suddenly and exponentially. What is interesting is that in both cases at those water contents, the size and the concentration of polymersomes reach already in nearly steady state. Then why the fluorescence intensity increases so abruptly? The first stage of fluorescence increase can be explained by the polymersome formation. The non-water-soluble P(TPE-TMC) block self-assembled into the core of membrane and the intramolecular motion of TPE moieties was restricted. But because of the presence of solvent (THF or dioxane) in the membrane, this restriction of motion is limited, therefore the fluorescence intensity is moderate. After 60% or 50% of water content, the sudden increase of fluorescence intensity upon further water addition could be caused by the removal of the organic solvent from the membrane. The concentration gradient of the organic solvent from inside to outside the membrane resulted in the release of THF or dioxane by osmotic pressure. Consequently, the AIEgens, *i.e.* TPE moieties, aggregated effectively. As there were few solvent molecules to "lubricate" the intramolecular motion, the photoluminescence was activated efficiently to give high fluorescence intensity. The turning point between these two stages appeared earlier in dioxane/water than in THF/water, because THF is a better solvent for P(TPE-TMC) than dioxane. Both polymersomes in pure water after dialysis against water show very strong fluorescence when excited by 365 nm UV light, as shown by their photographs under UV (insets in Figure 5A and Figure 5B). Their quantum yield was measured as 12.7% using the method described in the literature[42] (see Supporting Information Equation S1).

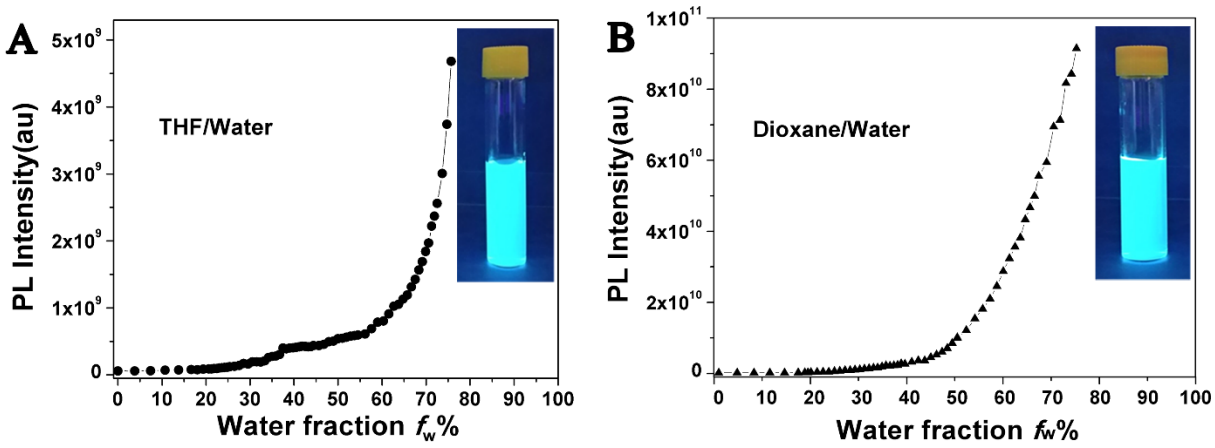

Figure 5. Evolution of fluorescence intensity as a function of water content during the polymersome formation. (A) THF/H_2O mixture. (B) Dioxane/H_2O mixture. Excitation wavelength is 382 nm. The photoluminescence (PL) intensity is the average intensity collected from the wavelength 473nm to 479nm. The two photographs in the insets correspond to the polymersome dispersions in pure water after dialysis against water when excited by UV light of 365 nm.

CONCLUSION

We have designed and synthesized a series of amphiphilic block copolymers PEG_{45}-*b*-P(TPE-TMC)$_n$ using ring opening polymerization catalyzed by organic catalysts. Their hydrophobic block is a biodegradable poly(trimethylenecarbonate) bearing tetraphenylethylene as side-groups. Bright AIE fluorescent polymersomes were prepared from PEG_{45}-*b*-P(TPE-TMC)$_n$ using nanoprecipitation methods. The effect of the co-solvent (THF or dioxane) and the effect of the length of hydrophobic block on the polymersome formation were studied in detail. For the self-assemblies of PEG_{45}-*b*-P(TPE-TMC)$_{13}$ in THF/water, the final average hydrodynamic diameter of polymersomes was around 250 nm; while it was around 650 nm in dioxane/water. The diameter of polymersomes decreased with the decrease of hydrophobic length and the increase of

hydrophilic ratio in the amphiphilic block copolymers PEG_{45}-*b*-$P(TPE\text{-}TMC)_n$. The average size of polymersomes changed from 450 nm, 250 nm, 90 nm to 70 nm when the degree of polymerization of $P(TPE\text{-}TMC)_n$ changed from n = 16, 13, 9 to 7.

The self-assembling process of PEG_{45}-*b*-$P(TPE\text{-}TMC)_{13}$ were followed *in situ* by DLS, cryo-EM and spectrofluorometer. Four events were found to be involved in the formation of polymersomes. Sheets and giant vesicles with D_h up to 3μm were formed at the first stage (with 20-32 wt% of water content in THF/water and 10-18 wt% of water in dioxane/water). Then the sheets tended to close to form vesicles and the large vesicles evolved into small ones (with 32-36 wt% of water content in THF and 18-25 wt% of water in dioxane/water). This second event was characterized by the sudden increase of the concentration and decrease of the size of polymersomes. The third event corresponded to the stabilization of the size and the concentration of polymersomes (with water content > 36 wt% in THF/water and > 25 wt% in dioxane/water). The fourth event corresponded to the removal of organic solvent from the P(TPE-TMC) membrane (starting at 60% water content in THF/water and 50% in dioxane/water) upon water addition. This event was characterized by the abrupt increase of the fluorescence intensity because of the strong restriction of intramolecular motion of TPE.

In summary, the membrane of polymersomes affords here a nanosized bright fluorescent system with self-assembly induced emission in the thickness scale of 10-15 nm. The polymersomes are formed *via* the closure of large bilayer lamellae self-assembled first by amphiphilic block copolymers. This mechanism can lead to high loading capacity of hydrophilic molecules inside the aqueous compartments of polymersomes. The control of the size of polymersomes by the choice of co-solvent (THF or dioxane) and by the design of suitable hydrophilic/hydrophobic ratio of block copolymers is of great importance for the control of the

cell uptake of polymersomes in the biotechnological applications. Therefore, the bright AIE polymersomes reported here can be potentially used as a stable fluorescent tool to monitor the transportation and distribution of drugs and bioconjugates in living cells.

EXPERIMENTAL SECTION

Materials. Diphenylmethane (99%, J&K Scientific), 4-methoxybenzophenone (97%, Accela), n-butyllithium (J&K Scientific), p-toluene sulfonic acid (PSTA, 98%, Beijing HWRK Chem. Co), boron tribromide (Acros), 1,6-dibromohexane (97%, Alfa Aesar), dimethylolpropionic acid (98%, Acros), triphosgene (Acros), dichloromethane, potassium hydroxide, acetonitrile, N, N-dimethyl formamide were used as received. Toluene was dried over sodium and distilled before using. Poly(ethylene glycol) methyl ether (known as mPEG-OH, M_n= 2000 g.mol^{-1}, J&K Scientific) was purified and dried before using. After three cycles of precipitation/filtration from diethyl ether, the solvent residues in mPEG-OH were evaporated under reduced pressure and the resulting solid was dried over P_2O_5 under vacuum for at least 4 days. N- (3,5-Trifluoromethyl) phenyl-N′-cyclohexylthiourea) (TU) was prepared according to a procedure reported previously.[33] TU was dissolved in dry tetrahydrofuran and dried over molecular sieves overnight. The mixture was filtered and the solvent removed in vacuo. 1, 8-Diazabicyclo [5,4,0]-undec-7-ene (DBU, 99%, Alfa Aesar) was dried over CaH_2 overnight, and dried DBU was obtained after vacuum distillation. Both TU and DBU were transferred to a glovebox before using.

Instruments. ^{1}H NMR and ^{13}C NMR spectra were measured on a Bruker AV 400 spectrometer. Weight-avreage molecular weight (Mw) and polydispersity (Mw/Mn) of the polymers were estimated by Size-exclusion chromatography (SEC) system. Tetrahydrofuran was used as eluent with a flow rate of 1 mL/min. UV spectra were measured on a Milton Ray

Spectronic 3000 Array spectrophotometer. Photoluminescence (PL) spectra were recorded on a PerkinElmer LS55 and Spex FluoroMax Spectrofluorometer. The solution spectra were recorded in solutions of THF or dioxane with concentrations of approximately 10^{-5} M in quartz cells with a pathlength of 1 cm. Average diameters of micelles and their size distributions in dioxane/H_2O, THF/H_2O or pure water were measured at 25 ^{o}C by Photon correlation spectroscopy (PCS, Malvern zetasizer 3000HS, UK) with a 633 nm laser. A 90^{o} scattering angle was used for all measurements. The stock solution was filtered into the scattering cell through 0.45 mm filter and equilibrated for 10 min before measurements. Cryo-EM images were acquired on a JEOL 2200FS energy-filtered (20 eV slit) field emission gun electron microscope operating at 200 kV using a Gatan US1000 camera. For the sample preparation, a total of 5 μL of samples were deposited onto a 200-mesh holey copper grid (Ted Pella Inc., U.S.A.) and flash-frozen in liquid ethane cooled down at liquid nitrogen temperature using a Leica CPC system.

Synthesis of Compound 2. A two-necked flask containing compound 1 (41.23 g, 113.74 mmol) and dried DCM (300 mL) was cooled to -20 °C, and BBr_3 (85.48 g, 341.22 mmol) was slowly added. The mixture was warmed to room temperature, allowed to stand for 4 h, and then poured into saturated aqueous sodium bicarbonate. The organic phase was dried over anhydrous Na_2SO_4, and the crude product obtained in nearly quantitative yield (38.23 g, 96.46%). ^{1}H NMR (400MHz, $CDCl_3$), δ (ppm): 7.01-7.13 (m, 15H, Ar*H*). 6.90 (d, J = 8.0 Hz, 2H, Ar*H*). 6.56 (d, J = 8.0 Hz, 2H, Ar*H*). 4.60 (s, 1H, O*H*). ^{13}C NMR (100MHz, $CDCl_3$), δ (ppm): 154.08, 144.12, 144.01, 140.54, 140.34, 136.54, 132.87, 131.49, 131.46, 127.84, 127.74, 126.52, 126.4, 114.72.

Synthesis of Compound 3. Compound 2 (23.73 g, 68.1 mmol) was dissolved in 200 mL of ACN, K_2CO_3 (14.2 g, 102.15 mmol) and 1,6-dibromohexane (83 g, 340.51 mmol) were added, and the mixture was refluxed for 4h before cooling and filtering. The filtrate was concentrated

and purified on a silica gel column with an eluent of petroleum ether and dichloromethane (1:1 v/v) to give product (30.36 g, 87%). 1H NMR (400MHz, $CDCl_3$), δ (ppm): 7.00-7.15 (m, 15H, Ar*H*). 6.94 (d, *J* = 9.0 Hz, 2H, Ar*H*). 6.63 (d, *J* = 9.0 Hz, 2H, Ar*H*). 3.89 (t, *J* = 6.44Hz, 2H, OCH_2), 3.43 (t, *J* = 6.92, 2H, CH_2Br), 1.86-1.93 (m, 2H, CH_2), 1.73-1.80 (m, 2H, CH_2), 1.48-1.52 (m, 4H, CH_2). ^{13}C NMR (100MHz, $CDCl_3$), *δ* (ppm): 157.72, 144.19, 144.14, 140.70, 140.16, 136.12, 132.65, 131.52, 131.49, 131.36, 127.83, 127.71, 126.46, 126.34, 113.70, 67.65, 33.92, 32.82, 29.26, 28.08, 25.46.

Synthesis of Compound 4. In a round bottom flask, compound 3 (18.47 g, 36.11mmol), 2,2-bis(methylol)propionic acid (7.26 g, 54.16 mmol) and potassium hydroxide (3.04 g, 54.16 mmol) were dissolved in 100 mL of DMF. The medium was stirred at 100 C for 15h. the KBr salt was filtered off and DMF was evaporated under vacuum. The residual was then recovered by extraction with DCM. The solvent was eliminated under vacuum to yield a light yellowish oil. Yield: 16.88g, 82.7%. ^{1}H NMR (400MHz, $CDCl_3$), *δ* (ppm): 7.00-7.15 (m, 15H, Ar*H*), 6.93 (d, *J* = 8.9 Hz, 2H, Ar*H*), 6.62 (d, *J* = 8.8 Hz, 2H, Ar*H*), 4.13 (t, *J* = 6.6Hz, 2H, COOCH_2), 3.86-3.93 (m, 4H, OCH_2 & CH_2OH), 3.69-3.74 (dd, J_1 = 6.2Hz, J_2 = 11.3Hz, 2H, CH_2OH), 2.93-2.91 (m, 2H, CH_2OH), 1.63-1.79 (m, 4H, CH_2), 1.39-1.53 (m, 4H, CH_2), 1.06 (s, 3H, CCH_3). ^{13}C NMR (100MHz, $CDCl_3$), *δ* (ppm): 176.13, 157.69, 144.17, 144.13, 144.11, 140.67, 140.14, 136.11, 132.63, 131.50, 131.47, 131.45, 127.82, 127.70, 126.45, 126.33, 113.66, 68.62, 67.63, 65.16, 49.21, 29.29, 28.58, 25.85, 25.79, 17.28.

Synthesis of TPE-TMC. Compound 4 (16.88 g, 29.89 mmol) was dissolved in DCM (150 mL) and pyridine (14.5 mL, 179.35 mmol) and the solution was chilled to −78°C under Ar. A solution of triphosgene (4.97 g, 16.74 mmol) in DCM (50 mL) was added dropwise over 0.5 h, at which point the reaction mixture was allowed to warm to room temperature for 2 h. The reaction

was quenched by addition of saturated aqueous NH_4Cl after which the organic layer was washed with 1 M aqueous HCl (3 times), saturated aqueous $NaHCO_3$, dried (MgSO4), filtered and evaporated to give product as a white solid (pinkish in some preparations) (12.65 g, 71.6%). ^{1}H NMR (400MHz, $CDCl_3$), δ (ppm): 6.99-7.14 (m, 15H, Ar*H*), 6.92 (d, J = 8.7 Hz, 2H, Ar*H*), 6.62 (d, J = 8.7 Hz, 2H, Ar*H*), 4.68 (d, J = 10.8Hz, 2H, OCOCH_2), 4.17-4.23 (m, 4H, COOCH_2&CH_2OCO), 3.88 (t, J = 6.3Hz, 2H, OCH_2), 1.67-1.79 (m, 4H, CH_2), 1.39-1.52 (m, 4H, CH_2), 1.32 (s, 3H, CCH_3). ^{13}C NMR (100MHz, $CDCl_3$), δ (ppm): 157.67, 147.54, 144.16, 144.11, 144.09, 140.65, 140.13, 136.10, 132.62, 131.49, 131.46, 131.44, 127.81, 127.69, 126.44, 126.32, 113.64, 73.14, 67.57, 66.35, 40.31, 29.25, 28.46, 25.83, 25.67, 17.75.

Polymerization. All the polymerizations were carried out under argon in a 10mL Schlenk tube equipped with a Teflon coated stirring bar. The typical polymerization procedure for homopolymer was as follows. In a glove box, catalyst DBU (1.93mg, 0.012mmol), initiator benzyl alcohol (0.9mg, 0.008mmol), monomer 1 (150mg, 0.25 mmol) and catalyst TU (4.7mg, 0.012mmol) were dissolved in toluene. The reaction mixture was stirred for 5h at room temperature. ^{1}H NMR analysis showed that the conversion of monomer was 85.8%. The toluene solution was then poured drop-by-drop into cold methanol (40mL) to precipitated the crude homopolymer. after dissolved in DCM and precipitated in methanol twice more, the purified polymer was collected and dried the under vacuum.

Preparation of Polymersomes. The polymersomes were prepared following a classical nanoprecipitation procedure as reported previously**.** The diblock copolymer was dissolved in 1 mL of THF or dioxane at a concentration of 0.25 wt%. 2 mL of deionized water was injected slowly at the rate of 3 μL/min with slight shaking. The whole process of nanoprecipitation was carried out at room temperature. The obtained turbid mixtures were then dialyzed against water

for 3 days to remove the THF or dioxane using a Spectra/Por regenerated cellulose membrane with a molecular weight cutoff (MWCO) of 3500 Da.

ASSOCIATED CONTENT

Supporting Information. ^{1}H NMR and ^{13}C NMR spectra of all compounds. SEC of the synthesized polymer. UV-vis spectra of monomer **TPE-TMC** and homopolymer **P(TPE-TMC)$_{24}$** and copolymer **PEG-*b*-P(TPE-TMC)$_{13}$**. This material is available free of charge *via* the Internet at http://pubs.acs.org

The authors declare no competing financial interest.

AUTHOR INFORMATION

Corresponding Author

Email: min-hui.li@chimieparistech.psl.eu (M.-H.LI.)

Author Contributions

The manuscript was written through contributions of all authors. All authors have given approval to the final version of the manuscript. † These authors contributed equally.

ACKNOWLEDGMENT

This work is supported by the National Natural Science Foundation of China (21604001 and 21528402) and the French National Research Agency (ANR-16-CE29-0028). Yujiao FAN thanks the China Scholarship Council for funding her PhD scholarship. We also acknowledge the PICT-IBiSA of Institut Curie for providing access to chemical imaging equipment.

REFERENCES

1. Discher, D. E.; Eisenberg, A., Polymer Vesicles. *Science* **2002,** *297*, 967-973.

2. Ahmed, F.; Pakunlu, R. I.; Brannan, A.; Bates, F.; Minko, T.; Discher, D. E., Biodegradable Polymersomes Loaded with both Paclitaxel and Doxorubicin Permeate and Shrink Tumors, Inducing Apoptosis in Proportion to Accumulated Drug. *J. Control. Release* **2006,** *116*, 150-158.
3. Du, J.; O'Reilly, R. K., Advances and Challenges in Smart and Functional Polymer Vesicles. *Soft Matter* **2009,** *5*, 3544–3561.
4. Le Meins, J. F.; Sandre, O.; Lecommandoux, S., Recent Trends in the Tuning of Polymersomes' Membrane Properties. *Eur. Phys. J. E* **2011,** *34*, 1-17.
5. Li, M.-H.; Keller, P., Stimuli-Responsive Polymer Vesicles. *Soft Matter* **2009,** *5*, 927-937.
6. Meng, F.; Zhong, Z.; Feijen, J., Stimuli-Responsive Polymersomes for Programmed Drug Delivery. *Biomacromolecules* **2009,** *10*, 197-209.
7. Duncan, T. V.; Ghoroghchian, P. P.; Rubtsov, I. V.; Hammer, D. A.; Therien, M. J., Ultrafast Excited-State Dynamics of Nanoscale Near-Infrared Emissive Polymersomes. *J. Am. Chem. Soc.* **2008,** *130*, 9773-9784.
8. Lai, M. H.; Lee, S.; Smith, C. E.; Kim, K.; Kong, H., Tailoring Polymersome Bilayer Permeability Improves Enhanced Permeability and Retention Effect for Bioimaging. *ACS Appl. Mater. Interfaces* **2014,** *6*, 10821-10829.
9. Smart, T.; Lomas, H.; Massignani, M.; Flores-Merino, M. V.; Perez, L. R.; Battaglia, G., Block Copolymer Nanostructures. *Nano Today* **2008,** *3*, 38-46.
10. Chen, M.; Yin, M., Design and Development of Fluorescent Nanostructures for Bioimaging. *Prog. Polym. Sci.* **2014,** *39*, 365-395.
11. Mei, J.; Leung, N. L.; Kwok, R. T.; Lam, J. W.; Tang, B. Z., Aggregation-Induced Emission: Together We Shine, United We Soar! *Chem. Rev.* **2015,** *115*, 11718-11940.
12. Ding, D.; Li, K.; Liu, B.; Tang, B. Z., Bioprobes Based on AIE Fluorogens. *Acc. Chem. Res.* **2013,** *46*, 2441-2453.
13. Liang, J.; Tang, B. Z.; Liu, B., Specific Light-up Bioprobes Based on AIEgen Conjugates. *Chem. Soc. Rev.* **2015,** *44*, 2798-2811.
14. Kwok, R. T.; Leung, C. W.; Lam, J. W.; Tang, B. Z., Biosensing by Luminogens with Aggregation-Induced Emission Characteristics. *Chem. Soc. Rev.* **2015,** *44*, 4228-4238.
15. He, L.; Liu, X.; Liang, J.; Cong, Y.; Weng, Z.; Bu, W., Fluorescence Responsive Conjugated Poly(tetraphenylethene) and its Morphological Transition from Micelle to Vesicle. *Chem. Commun.* **2015,** *51*, 7148-7151.
16. Huo, M.; Ye, Q.; Che, H.; Wang, X.; Wei, Y.; Yuan, J., Polymer Assemblies with Nanostructure-Correlated Aggregation-Induced Emission. *Macromolecules* **2017,** *50*, 1126-1133.
17. Li, J.; Liu, K.; Chen, H.; Li, R.; Drechsler, M.; Bai, F.; Huang, J.; Tang, B. Z.; Yan, Y., Functional Built-In Template Directed Siliceous Fluorescent Supramolecular Vesicles as Diagnostics. *ACS Appl. Mater. Interfaces* **2017,** *9*, 21706-21714.
18. Wang, X.; Yang, Y.; Yang, F.; Shen, H.; Wu, D., pH-Triggered Decomposition of Polymeric Fluorescent Vesicles to Induce Growth of Tetraphenylethylene Nanoparticles for Long-Term Live Cell Imaging. *Polymer* **2017,** *118*, 75-84.
19. Wang, X.; Yang, Y.; Zuo, Y.; Yang, F.; Shen, H.; Wu, D., Facile Creation of FRET Systems from a pH-Responsive AIE Fluorescent Vesicle. *Chem. Commun.* **2016,** *52*, 5320-5323.
20. Zhang, M.; Yin, X.; Tian, T.; Liang, Y.; Li, W.; Lan, Y.; Li, J.; Zhou, M.; Ju, Y.; Li, G., AIE-Induced Fluorescent Vesicles Containing Amphiphilic Binding Pockets and the FRET Triggered by Host-Guest Chemistry. *Chem. Commun.* **2015,** *51*, 10210-10213.
21. Zhao, Y.; Wu, Y.; Yan, G.; Zhang, K., Aggregation-Induced Emission Block Copolymers Based on Ring-Opening Metathesis Polymerization. *RSC Adv.* **2014,** *4*, 51194-51200.

22. Chen, W.; Meng, F.; Cheng, R.; Deng, C.; Feijen, J.; Zhong, Z., Advanced Drug and Gene Delivery Systems Based on Functional Biodegradable Polycarbonates and Copolymers. *J. Control. Release* **2014,** *190*, 398-414.
23. Fukushima, K., Poly(trimethylene carbonate)-Based Polymers Engineered for Biodegradable Functional Biomaterials. *Biomater. Sci.* **2016,** *4*, 9-24.
24. Sanson, C.; Schatz, C.; Le Meins, J. F.; Brulet, A.; Soum, A.; Lecommandoux, S., Biocompatible and Biodegradable Poly(trimethylene carbonate)-b-Poly (L-glutamic acid) Polymersomes: Size Control and Stability. *Langmuir* **2010,** *26*, 2751-2760.
25. Li, S. K.; Meng, F. H.; Wang, Z. J.; Zhong, Y. N.; Zheng, M.; Liu, H. Y.; Zhong, Z. Y., Biodegradable Polymersomes with An Ionizable Membrane: Facile Preparation, Superior Protein Loading, and Endosomal pH-Responsive Protein Release. *Eur. J. Pharm. Biopharm.* **2012,** *82*, 103-111.
26. Zhou, L.; Zhang, D.; Hocine, S.; Pilone, A.; Trépout, S.; Marco, S.; Thomas, C.; Guo, J.; Li, M.-H., Transition from Smectic Nanofibers to Smectic Vesicles in the Self-Assemblies of PEG-b-Liquid Crystal Polycarbonates. *Polym. Chem.* **2017,** *8*, 4776-4780.
27. Dove, A. P., Organic Catalysis for Ring-Opening Polymerization. *ACS Macro Lett.* **2012,** *1*, 1409-1412.
28. Nederberg, F.; Lohmeijer, B. G. G.; Leibfarth, F.; Pratt, R. C.; Choi, J.; Dove, A. P.; Waymouth, R. M.; Hedrick, J. L., Organocatalytic Ring Opening Polymerization of Trimethylene Carbonate. *Biomacromolecules* **2007,** *8*, 153-160.
29. Nederberg, F.; Trang, V.; Pratt, R. C.; Mason, A. F.; Frank, C. W.; Waymouth, R. M.; Hedrick, J. L., New Ground for Organic Catalysis: A Ring-Opening Polymerization Approach to Hydrogels. *Biomacromolecules* **2007,** *8*, 3294-3297.
30. Kamber, N. E.; Jeong, W.; Waymouth, R. M.; Pratt, R. C.; Lohmeijer, B. G. G.; Hedrick, J. L., Organocatalytic Ring-Opening Polymerization. *Chem. Rev.* **2007,** *107*, 5813-5840.
31. Venkataraman, S.; Lee, A. L.; Maune, H. T.; Hedrick, J. L.; Prabhu, V. M.; Yang, Y. Y., Formation of Disk- and Stacked-Disk-like Self-Assembled Morphologies from Cholesterol-Functionalized Amphiphilic Polycarbonate Diblock Copolymers. *Macromolecules* **2013,** *46*, 4839-4846.
32. Tempelaar, S.; Mespouille, L.; Coulembier, O.; Dubois, P.; Dove, A. P., Synthesis and Post-Polymerisation Modifications of Aliphatic Poly(carbonate)s Prepared by Ring-Opening Polymerisation. *Chem. Soc. Rev.* **2013,** *42*, 1312-1336.
33. Sanders, D. P.; Fukushima, K.; Coady, D. J.; Nelson, A.; Fujiwara, M.; Yasumoto, M.; Hedrick, J. L., A Simple and Efficient Synthesis of Functionalized Cyclic Carbonate Monomers Using a Versatile Pentafluorophenyl Ester Intermediate. *J. Am. Chem. Soc.* **2010,** *132*, 14724-14726.
34. Kim, S. H.; Tan, J. P.; Fukushima, K.; Nederberg, F.; Yang, Y. Y.; Waymouth, R. M.; Hedrick, J. L., Thermoresponsive Nanostructured Polycarbonate Block Copolymers as Biodegradable Therapeutic Delivery Carriers. *Biomaterials* **2011,** *32*, 5505-5514.
35. Tong, H.; Hong, Y. N.; Dong, Y. Q.; Haeussler, M.; Li, Z.; Lam, J. W. Y.; Dong, Y. P.; Sung, H. H. Y.; Williams, I. D.; Tang, B. Z., Protein Detection and Quantitation by Tetraphenylethene-Based Fluorescent Probes with Aggregation-Induced Emission Characteristics. *J. Phys. Chem. B* **2007,** *111*, 11817-11823.
36. Yang, J.; Pinol, R.; Gubellini, F.; Levy, D.; Albouy, P. A.; Keller, P.; Li, M.-H., Formation of Polymer Vesicles by Liquid Crystal Amphiphilic Block Copolymers. *Langmuir* **2006,** *22*, 7907-7911.

37. Grassucci, R. A.; Taylor, D. J.; Frank, J., Preparation of Macromolecular Complexes for Cryo-Electron Microscopy. *Nat. Protoc.* **2007,** *2*, 3239-46.
38. Zeng, W.; Du, Y.; Xue, Y.; Frisch, H. L., Solubility Parameters. In *Physical Properties of Polymers Handbook*, Mark, J. E., Ed. Springer New York: New York, NY, 2007; pp 289-303.
39. Blanazs, A.; Armes, S. P.; Ryan, A. J., Self-Assembled Block Copolymer Aggregates: From Micelles to Vesicles and their Biological Applications. *Macromol. Rapid Commun.* **2009,** *30*, 267-277.
40. Jia, L.; Albouy, P.-A.; Di Cicco, A.; Cao, A.; Li, M.-H., Self-Assembly of Amphiphilic Liquid Crystal Block Copolymers Containing a Cholesteryl Mesogen: Effects of Block Ratio and Solvent. *Polymer* **2011,** *52*, 2565-2575.
41. Gaumet, M.; Vargas, A.; Gurny, R.; Delie, F., Nanoparticles for Drug Delivery: The Need for Precision in Reporting Particle Size Parameters. *Eur. J. Pharm. Biopharm*. **2008**, *69*, 1-9.
42. Lu, H.; Su, F.; Mei, Q.; Tian, Y.; Tian, W.; Johnson, R. H.; Meldrum, D. R., Using Fluorine-Containing Amphiphilic Random Copolymers to Manipulate the Quantum Yields of Aggregation-Induced Emission Fluorophores in Aqueous Solutions and the Use of These Polymers for Fluorescent Bioimaging. *J. Mater. Chem*. **2012**, *22*, 9890-9900.

TOC Graphic

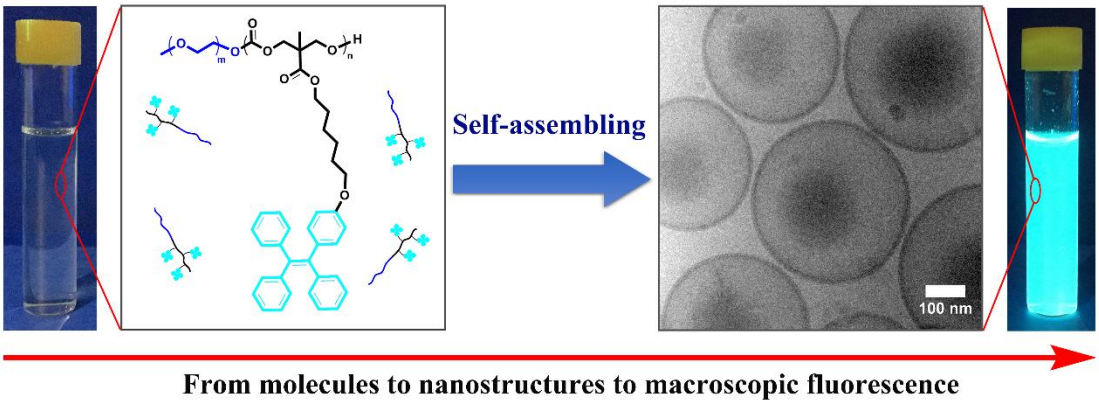

For Table of Contents Only